

# Simulations of morphological transformation in silver nanoparticles as a tool for assessing their reactivity and potential toxicity

Martin, Paul; Zhang, Peng; Rodger, P. Mark; Valsami-Jones, Eugenia

DOI:

[10.1016/j.impact.2019.100147](https://doi.org/10.1016/j.impact.2019.100147)

[10.1016/J.IMPACT.2019.100147](https://doi.org/10.1016/J.IMPACT.2019.100147)

License:

Creative Commons: Attribution-NonCommercial-NoDerivs (CC BY-NC-ND)

*Document Version*

Peer reviewed version

*Citation for published version (Harvard):*

Martin, P, Zhang, P, Rodger, PM & Valsami-Jones, E 2019, 'Simulations of morphological transformation in silver nanoparticles as a tool for assessing their reactivity and potential toxicity', *NanoImpact*, vol. 14, 100147. <https://doi.org/10.1016/j.impact.2019.100147>, <https://doi.org/10.1016/J.IMPACT.2019.100147>

[Link to publication on Research at Birmingham portal](#)

**Publisher Rights Statement:**

Checked for eligibility: 15/03/2019

**General rights**

Unless a licence is specified above, all rights (including copyright and moral rights) in this document are retained by the authors and/or the copyright holders. The express permission of the copyright holder must be obtained for any use of this material other than for purposes permitted by law.

- Users may freely distribute the URL that is used to identify this publication.
- Users may download and/or print one copy of the publication from the University of Birmingham research portal for the purpose of private study or non-commercial research.
- User may use extracts from the document in line with the concept of 'fair dealing' under the Copyright, Designs and Patents Act 1988 (?)
- Users may not further distribute the material nor use it for the purposes of commercial gain.

Where a licence is displayed above, please note the terms and conditions of the licence govern your use of this document.

When citing, please reference the published version.

**Take down policy**

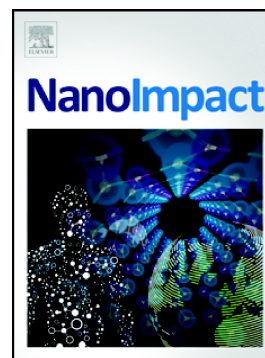
While the University of Birmingham exercises care and attention in making items available there are rare occasions when an item has been uploaded in error or has been deemed to be commercially or otherwise sensitive.

If you believe that this is the case for this document, please contact [UBIRA@lists.bham.ac.uk](mailto:UBIRA@lists.bham.ac.uk) providing details and we will remove access to the work immediately and investigate.

## Accepted Manuscript

Simulations of morphological transformation in silver nanoparticles as a tool for assessing their reactivity and potential toxicity

Paul Martin, Peng Zhang, P. Mark Rodger, Eugenia Valsami-Jones



PII: S2452-0748(18)30183-6  
DOI: <https://doi.org/10.1016/j.impact.2019.100147>  
Article Number: 100147  
Reference: IMPACT 100147  
To appear in: *NANOIMPACT*  
Received date: 2 November 2018  
Revised date: 14 February 2019  
Accepted date: 21 February 2019

Please cite this article as: P. Martin, P. Zhang, P.M. Rodger, et al., Simulations of morphological transformation in silver nanoparticles as a tool for assessing their reactivity and potential toxicity, *NANOIMPACT*, <https://doi.org/10.1016/j.impact.2019.100147>

This is a PDF file of an unedited manuscript that has been accepted for publication. As a service to our customers we are providing this early version of the manuscript. The manuscript will undergo copyediting, typesetting, and review of the resulting proof before it is published in its final form. Please note that during the production process errors may be discovered which could affect the content, and all legal disclaimers that apply to the journal pertain.

# Simulations of Morphological Transformation in Silver Nanoparticles as a Tool for Assessing their Reactivity and Potential Toxicity

Paul Martin,<sup>1</sup> Peng Zhang,<sup>1</sup> P. Mark Rodger,<sup>2</sup> and Eugenia Valsami-Jones<sup>1\*</sup>

<sup>1</sup> School of Geography, Earth and Environmental Sciences, University of Birmingham,  
Edgbaston, Birmingham B15 2TT, UK

<sup>2</sup> Department of Chemistry, University of Warwick, Coventry CV4 7AL, UK

**ABSTRACT:** Concerns about the safety of engineered nanomaterials have not yet been addressed in a systematic way, despite many years of nanotoxicology research. Here we present a computational approach that allows predictions of nanomaterial reactivity as an indicator for toxicity; the approach is powerful, as it is based on fundamental structural criteria, but we also demonstrate that predictions from the simulations fit well with experimentally observed nanoparticle behaviour. Using molecular dynamic simulations, the study predicts surface structures and energetics of silver nanoparticles (AgNPs), which enable an assessment of the impact of water molecules on the surface transformation of AgNPs; the latter controls their behaviour in aqueous media and ultimately their transport, fate, and toxicity. The work shows that size exerts an important control on reactivity and likely also toxicity, a concept proposed at the start of the nanotoxicology debate, but never demonstrated at the smaller end of the nanoscale, or at a systematically resolved range of sizes. A key observation is that experimentally imperceptible differences in size may stabilise structures with hugely different reactivities. We build our framework using AgNPs, but stipulate this can be easily extended to other NP structures and chemistries and expanded to include interactions with biomolecules.

**KEYWORDS:** silver nanoparticle; Morphological transformation; size; toxicity; computational simulation

## 1. Introduction

Nanotechnology has the potential to revolutionise our future, offering life-saving or climate-protecting applications and being part of a multitude of current technological developments from aerospace technologies to food packaging and cosmetics (Nafisi and Maibach, 2017; Barako et al., 2018; Pereda et al., 2018). Failure of nanotechnology to realise its potential is inconceivable in terms of a financial and social impact, and yet, this prospect is not unlikely. Nanotechnology is currently being developed without full consideration of the safety aspects of the novel materials it creates, primarily due to difficulties in translating ‘traditional’ toxicology and ecotoxicology assessment protocols to equivalent methods suitable for nanomaterials, but also due to the difficulties inherent in the study of such small objects, which still lie at or below the detection limit of many established characterisation techniques.

The novelty of nanomaterials stems from their small size resulting in unique physical/chemical properties that differ from their bulk counterparts, either due to quantum effects, only occurring at the nanoscale, or their high surface to volume ratio that renders them more reactive even at the same mass dose. These unique properties may also give rise to safety concerns, as they can influence interactions with biota in ways that we cannot currently predict with confidence (Berhanu and Valsami-jones, 2012; Lynch et al., 2017; Briffa et al., 2018). The field of “nanotoxicology” (or “nanosafety”) aims to better understand nano-bio interactions and address concerns about nanomaterial safety (Maynard, 2014). Significant progress has been made in the past 15 years on the mechanistic understanding of nanotoxicity, and new advanced tools (e.g. high throughput toxicity testing, well-described nanomaterial libraries, systems biology based interpretations of toxicity effects) are emerging from a number of large scale projects addressing nanosafety (Fadeel et al., 2018). A platform that can assess the potentially endless combination

of nanomaterial structures in a systematic and reproducible way will allow reduction of the time required to assess each material/product. Therefore, although high-throughput toxicity testing will, in time, provide this platform, governments and industry need answers sooner. It is also essential to develop a predictive mechanistic understanding of which nanomaterial properties may be linked to increased toxicity to give society confidence in future legislation and enable industry to practise “safety-by-design” concepts (Lynch et al., 2014b) in future generations of nanomaterials. This can only be achieved when a structure-activity framework is established, as is available for pharmaceuticals (Perkins et al., 2003) based on the primary physicochemical properties of nanomaterials, linked to adverse outcome pathways.

Silver ions are well known for their antibacterial activity. In recent years, silver nanoparticles (AgNPs) have also been found to be toxic (Johnston et al., 2010; Khan et al., 2015; Dong et al., 2017; Li et al., 2017); it has been proposed that the particles alongside Ag ions produced from their dissolution, act in tandem to cause this effect, although alternative hypotheses (e.g. that toxicity is due to ionic Ag only) have also been proposed (Levard et al., 2012; De Matteis et al., 2015). Structural transformations of NPs are crucial for their physicochemical properties which determine their reactivity and toxicity (Wang et al., 2011; Zhu et al., 2012).

A body of experimental data exist on small AgNP dissolution (Peretyazhko et al., 2014; Ma et al., 2012) and on toxicity, particularly as this may be influenced by a protein corona forming around the particles (Durán et al., 2015).

The work presented here focuses on a different approach, starting from AgNPs fundamental characteristics (surface-properties, shape, thermodynamics), which are crucial for functionality and then using molecular simulations to predict their physicochemical response. Firstly, we

investigate nanostructural transformations in AgNPs by systematically examining morphology changes as a function of particle size (determined as number of atoms), at a much higher resolution that could be experimentally feasible; we then link these with surface-water interactions and establish their effect on shape, surface area and morphology. This work enables an alignment between nanoscale effects and nanoparticle activity, and considers how these morphology transformations help our understanding of potential toxicity and/or environmental impact of nanomaterials. Finally, predictions regarding nanoparticle structure-reactivity are placed in the context of toxicity data from the literature. Our work establishes a framework linking nanoparticle properties to toxicity at a computational scale, and crucially recognises fundamental and novel patterns of size related toxicity. As such it has the potential to contribute towards a safer and wider application of nanotechnology.

## **2. Materials and Methods**

### *2.1. Ag-Ag Interaction*

The Embedded Atom Model (EAM), Sutton and Chen many-body force field (Sutton and Chen, 1990) was used for the metal-metal interactions. Potentials of EAM type have been used to model a variety of properties of metals, including bulk properties (elastic constants and structural energy differences), point defect properties (vacancy and interstitial formation energy and activation energy of vacancy diffusion), planar defect properties (stacking fault energy, surface energy, surface relaxation, and reconstruction), and thermal properties (thermal expansion coefficients, specific heat, melting points, and heat of melting) (Lee et al., 2003; Medasani et al., 2007).

### *2.2 Water–Water Interaction.*

The flexible water model TIP3P/FS (Schmitt and Voth, 1999) (that is employed in the multistate EVB (MS-EVB) model (Day et al., 2002) was used in the solvated systems. It has the advantages of being computationally inexpensive, and of using the same parameters that are employed in the AMBER (Smith and Forester, 1996) force-field, so making it more straight forward to add organic molecules in future work.

### 2.3. Ag–Water Interaction

Consistent with the strategy adopted for interactions involving water in the General Amber Force Field (GAFF), (Wang et al., 2004) Lorentz–Berthelot mixing rules were used to derive the Lennard Jones interaction for interactions between silver and water. This results in no Ag–H interactions, while  $(\sigma, \epsilon) = (3.25 \text{ \AA}, 4.60 \text{ kJ mol}^{-1})$  for Ag–O<sub>(w)</sub>

### 2.4. Nanoparticle Simulations

*Vacuum Simulations:* METADISE (Toby Kelsey and áde Leeuw, 1996) was used to construct 30 different nanoparticles with sizes spanning the range 19–45,563 atoms, (roughly 1–20 nm). Each nanoparticle was then equilibrated using a simulated annealing (Barnard, 2010) protocol adapted from one developed recently for metallic nanoparticles. Initially, molecular dynamics simulations were performed on the particle in vacuum at a temperature  $T = 1200 \text{ K}$  to ensure complete melting of the nanoparticle; at the end of this simulation, there was no residual crystalline order, and the morphology of the particle bore no resemblance to that constructed with METADISE. The particle was then simulated at a series of lower temperatures ( $\Delta T = 100 \text{ K}$ ) with the final simulation being at  $T = 100 \text{ K}$ . The duration of each simulation stage depended on the size of cluster,  $N$ : at each temperature the trajectory time was 20 ns for  $N < 2000$ , 10 ns for  $2000 < N < 10\,000$ , and 4 ns for  $N > 10\,000$ . All molecular dynamics simulations were implemented using DL\_POLY classic, (Smith and Forester, 1996) and were



conducted at constant temperature using the Nosé-Hoover thermostat (Nosé, 1984; Hoover, 1985) with relaxation constant of 0.1 ps. Equations of motion were integrated with a timestep of 1 fs. The final simulation at 100 K was used for analysis, all reported properties were found to be stable during these simulations.

*Aqueous Simulations:* Explicit water molecules were added to a simulation cell containing the final configuration of the annealed structures described above. Periodic boundary conditions were used in these calculations and the dimensions of the simulation cell were chosen so that for the largest simulations there was at least 20 Å of water separating nanoparticle images across the periodic boundaries. A stepwise method for adding the water to our simulations was adopted. This involved fixing the nanoparticle in the centre of the box and overlaying a water simulation cell taken from an equilibrium simulation at  $T = 300$  K and  $P = 1$  bar. Water within 3 Å of any of the atoms in the nanoparticle was then removed and a 10 ps *NVT* MD simulation run to allow the water to relax around the AgNP. This process was then iterated, with an addition constraint that additional water could not be within 2 Å of existing water molecules, until no further water could be added to the system. This leads to simulation cells containing between 2440 and 16356 water molecules. Equilibration simulations, in which both Ag and water atoms were mobile, were then run for 1 ns using an *NPT* ensemble; during equilibration the dimensions of the simulation cell changed by less than 1%, with relaxation complete before the end of the simulation.

*Analysis:* Surface energies were calculated here by taking the total configuration energy of the nanoparticle and subtracting from this the equivalent bulk structure energy, for the same number of atoms. We then divide this by the total surface area of the nanoparticle to give the surface energy of the nanoparticle.

Contact and solvent accessible surface areas and volumes were calculated using Discovery Studio 3.1 (DS 3.1) Visualizer.(Accelrys Software Inc., 2013) Where a fixed probe radius was required, this was set to 1.40 Å, which is commonly used to represent water as the solvent.

In line with biochemical and biophysical studies (Lewis and Rees, 1985; Renthall, 1999; Kaczor et al., 2012), the surface fractal dimension,  $D_f$ , was defined from the expected scaling of surface area,  $A_s$ , with probe radius,  $r$ :

$$A_s = A_0 r^{2-D_f}$$

The 2 in the power reflects the fact that this variation is superimposed on the expected  $r^2$  dependence with nanoparticle (as opposed to probe) radius. Calculations were performed for probe radii in the range 1–2 Å, and showed good linearity (SI, S3: Calculating fractal dimension).

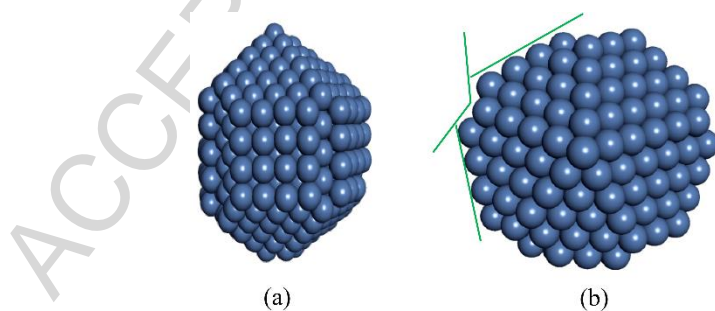
## 2. Results and discussion

Firstly, we consider morphological modifications predicted to occur in AgNPs as a function of size. Predictions are made by computationally “annealing” AgNPs (i.e. melting and then cooling in stages to below the freezing point) to find physically significant stable atomic configurations within a relevant range of nanoscale “sizes” (Varty, 2017). We thereby calculate the optimal distribution of atoms in the annealed particles and assess the structure of this most stable configuration (Table S1).

Structural-optimization by simulated annealing over an array of starting structures indicates that the final stable structure undergoes a morphological transition from icosahedral (19-225 atoms) to truncated-decahedral (489-3805 atoms) then to truncated-octahedral (4249-6603

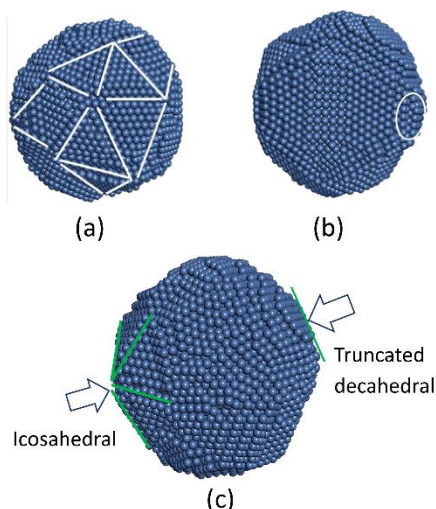
atoms) and finally to multifaceted, irregular sphere-like structures ( $>10,000$  atoms) as the size of the nanoparticle increases ( $19\text{--}45563$  atoms  $\approx 0.2\text{--}20\text{nm}$  in diameter). Similar structure variations with size were predicted in previous studies (Wang et al., 2011), but over a smaller size-range and, importantly, missing the larger particles which correspond to the size range of the majority of experimental approaches in nanotoxicology.

The larger size-range studied made it possible to observe that some of the AgNP shapes can be more strictly assigned than others. More specifically, some of the smaller AgNPs (eg., 19, 201, 225, and 249 atoms) clearly display icosahedral structures and the 489 atom AgNP has well-defined Marks decahedral morphology (Figure 1) (Marks, 1983); however, some other smaller AgNPs can only be approximately described as icosahedral. Furthermore, some of the larger AgNP modelled also show hybrid structures, where part is icosahedral and part is truncated-octahedral; we argue here that this may have a fundamental effect on potential reactivity as will be discussed later, after further hybrid/“poly”crystal structures are described and calculations of their surface-energy are presented.



**Figure 1.** 489 atom Silver Nanoparticle, a Marks' decahedral morphology. (a) Side elevation and (b) plan elevation. Green lines in (b) have been added to mark out the definite concave facets at the twin boundaries that define and illustrate that it is indeed a Marks' decahedral morphology.

Further, larger hybrid/“poly”crystal structures were identified which showed two alternative structures (one at 1961/3805 atoms and another at 2255/10425 atoms, Table S1). Each hybrid is distinctly different from those that are wholly icosahedral, truncated-decahedral, truncated-octahedral or irregular. Upon examination these specific models showed an overall structure made up of two distinct domains that are similar in size. The hybrid structures for 1961/3805 atom nanoparticles are mixes of truncated-decahedron and truncated-octahedron. The 2255/10425 atom particles are half icosahedron and half truncated-decahedron (Figure 2) with a clear structural split into two hemi-spherical domains. In these AgNPs it is clear that two crystal nucleation events occurred within the one nanoparticle. It is interesting to speculate about the lifetime of these “poly”crystal structures and how long it would be before the more stable form would win through and to further speculate on potential toxicity. The dual nucleations were evident at temperatures as high as 700 K, and were stable through the subsequent cooling stages and production simulation (up to 28 ns). We also note that their formation was not infrequent and thus their properties would influence the overall behaviour of AgNPs within the relevant size ranges. It is more difficult to place an upper bound on the longevity of such structures, but this is probably not insignificant, especially if exposed to environmental/biological media and potentially stabilised by organic coronas (Lynch et al., 2014a).



**Figure 2.** The 10425 atom silver nanoparticle, showing one hemisphere (a) that is icosahedral in character (with the 5 triangular  $\{111\}$  facets meeting at the central point), and the other hemisphere (b) that is truncated-decahedral, showing distinctly different character with  $\{100\}$  and  $\{111\}$  facets appearing adjacent in this 2<sup>nd</sup> hemisphere; (c) gives a side view showing the junction of the two distinct characters. At the meeting of the two hemispheres an irregular mix of morphology is formed, as seen within the white rectangle.

Careful analysis of the data shows one further transition between the truncated decahedral/octahedral structures, demonstrated by the 489 atom AgNP, where its shape has the well documented specific Marks decahedral hybrid morphology (Figure 1). Similar predictions of Marks morphologies for similarly sized silver clusters and 891 atom gold clusters have been made (Marks, 1983). It is clear that the number of atoms (effectively size) in the nanoparticle affects the resulting stable structure, be it icosahedral, truncated-decahedral, Marks decahedral, truncated-octahedral, spherical, half-half mixes, or irregular in shape.

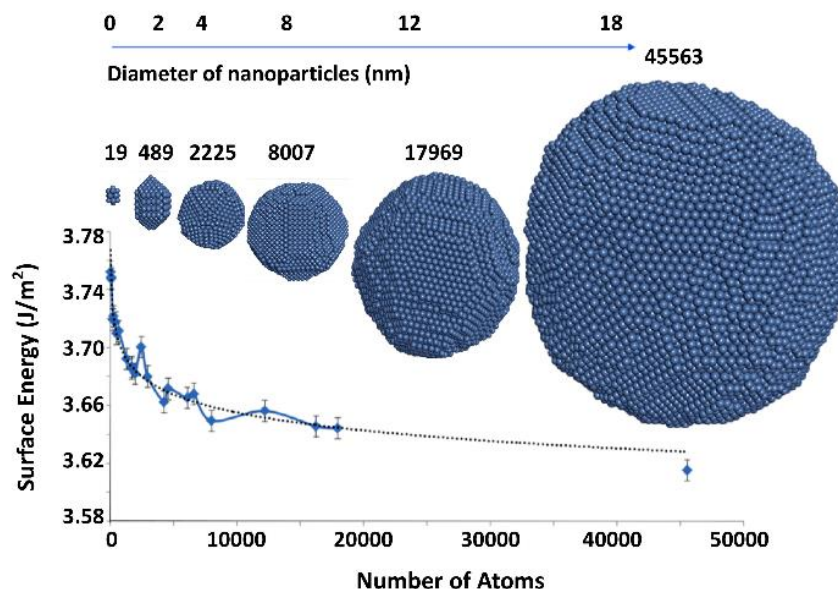
Another property relevant to nanoparticle-toxicity is the nanoparticle surface-energy ( $\gamma$ ), which provides an estimate of relative-stability and potential-reactivity. The literature values of  $\gamma$  for

AgNPs vary considerably depending on the specific experimental or theoretical approach. For example, work using the Kelvin equation (Nanda et al., 2002) reported  $\gamma=7.2 \text{ J/m}^2$  for free AgNPs (Nanda et al., 2003), whereas *ab initio* calculations give  $\gamma$  in the range  $1.0\text{--}2.2 \text{ J/m}^2$  (Todd and Lynden-Bell, 1993). The discrepancies may be due to the fundamental differences of the two methodological approaches. Figure 3(a) shows  $\gamma$  generally decreasing with increasing diameter, meaning the smaller icosahedral and truncated-decahedral structures are less stable, the truncated-octahedral structures are more stable, and the more irregular, multifaceted and sphere-like structures are most stable. Our calculated  $\gamma$  values range from  $3.75 \text{ J.m}^{-2}$  for the smallest AgNP to a minimum of  $3.55 \text{ J.m}^{-2}$  for the 35000 atom AgNP. This range falls between previous predictions (Todd and Lynden-Bell, 1993; Nanda et al., 2002; Nanda et al., 2003). Figure 3(b) focuses on  $\gamma$  predictions for the smaller AgNPs, containing less than 12000 atoms and having a diameter less than 8nm. This size range is where we predict the four hybrid structures; these hybrid structures show anomalous elevated surface energies. Formation of these hybrids at 1961, 2255, 3805 and 10425 atoms results in structures that are less energetically stable than the other nanoparticles, have higher  $\gamma$  and so are expected to be more reactive. We discuss this in more detail below, but note at this stage that an implication of this may be that reactivity/toxicity can vary substantially even though the size varies almost imperceptibly for current analytical capabilities.

Previous work gives relative thermodynamic stability (defined by  $\gamma$ ) for low-index silver surfaces as  $\{111\} > \{100\} > \{110\}$  (Todd and Lynden-Bell, 1993). This is consistent with the percentage abundance of these facets found for each AgNP in the present study (Table S2). The data also show that as AgNP size increases, there is a gradual increase in the % composition of  $\{111\}/\{110\}$  surfaces and concomitant decrease in % composition of  $\{100\}$  surfaces. Although

the overall effect is subtle, it is notable that certain configurations produce positive or negative “spikes” which are anomalous to the general pattern. For example the 1<sup>st</sup> such spike anomaly for the higher % of {111}/{100} surfaces and substantially lower % {110} surface occurs with the 489 atom Marks structure AgNP; the other spikes match  $\gamma$  anomalies shown in Figure 3(b). These anomalies mean that medium-stable {100} surfaces can represent as much as 45% of the total surface area or as little as 10% and the least stable {110} surface can represent as much as 25% or as little as 5%. As a result, the transitions from a high to low proportion of unstable surfaces can occur whilst size changes by just a couple of nanometers. This implicates that a significant change in exposed facets can occur while size varies almost undetectably. The change of facets could have a significant impact on the reactivity and toxicity of NPs which have been revealed by a few recent studies (Ge et al., 2016; Liu et al., 2016; Zhang et al., 2017).

Nanoparticles in water, particularly when they are charge stabilised, can easily lose their surface ligands, e.g. by displacement, or surface dissolution; furthermore, nanoparticles in contact with biological fluids are rapidly covered by biomolecules to form a corona that interacts with biological systems (Lynch et al., 2014a; Briffa et al., 2018); however because the corona is not at thermodynamic equilibrium, its composition/organization may fluctuate, again leaving exposed particle surfaces (Walczyk et al., 2010; Lartigue et al., 2012; Monopoli et al., 2012). Also, some AgNP synthesis methods do not involve the use of stabilising ligands, and bare AgNPs are often produced. It is therefore important that considerations of nanoparticle reactivity begin by assessing the effects of water around exposed silver surfaces, and so we investigate whether water can have an influence on the structure of a metallic nanoparticle and, in particular, predict the likely effects on surface facets.








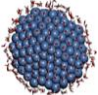
**Figure 3.** Surface energies for different sized silver nanoparticles over the whole range of sizes studied. Morphologies typical of the size ranges are depicted, which also gives a particle radius scale (top) to complement the use of number of atoms, for the horizontal axis.

The Methods section describes how explicit water molecules were added to annealed structures (Figure S1). Having established earlier the size effects on faceting, we now focus on how this may be modified in the presence of water. The simulations are used to predict the number of water molecules in the first hydration layer, the number of Ag surface atoms (water vs vacuo), and the proportion of the less stable  $\{100\}$  (water vs vacuo) (Table 1). The latter shows that water affects surface morphology, as the proportion of  $\{100\}$  changes on immersion in water. While visually the AgNP morphology appears similar in water and *in vacuo* (and hence only one image is given in Table 1), detailed inspection shows there are quantitative differences. In particular, there is an increase of between 2.6%–16.6% in the proportion of the AgNP surface that is made up of the less stable  $\{100\}$  facet when the AgNP is in contact with water. This is accompanied by no change in the percentage area of  $\{110\}$  surface, and thus a reduction in the

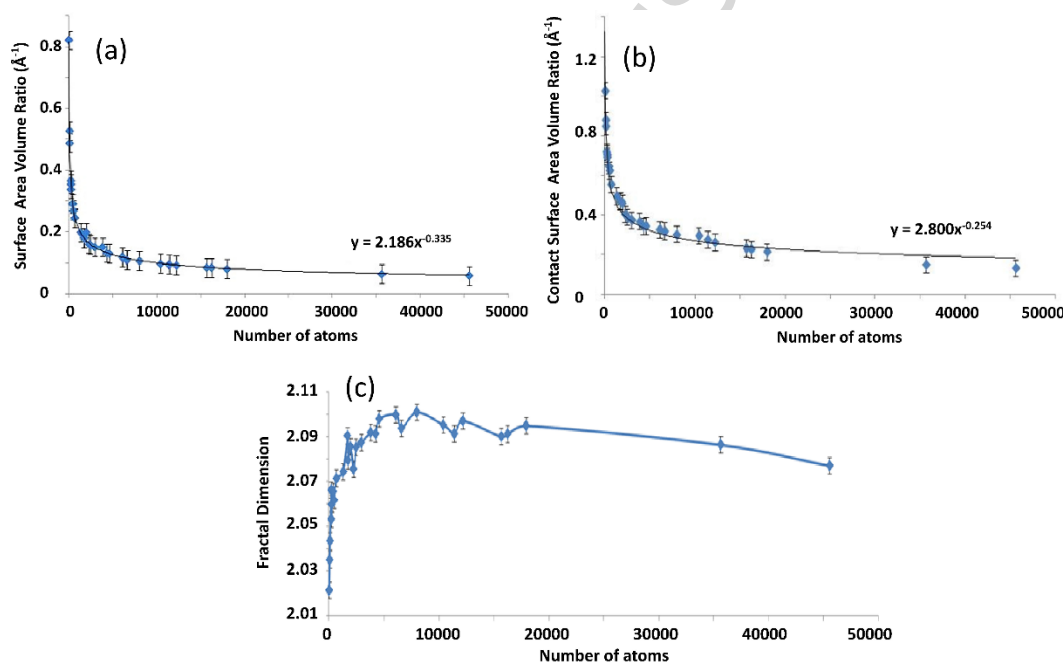


prominence of {111} and irregular surfaces. The one anomaly is the 489 Marks decahedron structure where there is no change for the percentage of atoms in the {100} facet structure. The reason for this could be that water molecules stabilise the concave facets present at the twin boundaries in the Marks decahedron, which then balances the further stabilisation of {100} facets seen in many of the other structures.

**Table 1.** Effect of water on the surface morphology of AgNPs. Percentage areas for the facets have been measured by counting the number of surface atoms; edge atoms (meeting at the interface between two low index surfaces) were split between the two surfaces according to the ratio of relative stability reported for low index surfaces for silver, calculated using the same interatomic potentials used in the current work.

| AgNP                                                                                      | No. of Ag atoms | No. of H <sub>2</sub> O molecules in 1 <sup>st</sup> hydration layer | No. of Ag surface atoms in AgNP in vacuo | % Ag {100} surface atoms in vacuo | No. of Ag surface atoms in AgNP in water | % Ag {100} surface atoms in water | % Change of {100} surface atoms |
|-------------------------------------------------------------------------------------------|-----------------|----------------------------------------------------------------------|------------------------------------------|-----------------------------------|------------------------------------------|-----------------------------------|---------------------------------|
| (i)    | 19              | 35                                                                   | 17                                       | n/a                               | 17                                       | n/a                               | n/a                             |
| (ii)   | 1961            | 680                                                                  | 663                                      | 45.2                              | 660                                      | 52.7                              | + 7.5 %                         |
| (iii)  | 4249            | 1254                                                                 | 1087                                     | 37.6                              | 1087                                     | 40.2                              | + 2.6 %                         |
| (iv)   | 11421           | 2288                                                                 | 2251                                     | 24.0                              | 2322                                     | 35.7                              | + 11.7 %                        |
| (v)    | 15683           | 2815                                                                 | 2891                                     | 15.0                              | 2883                                     | 31.6                              | + 16.6 %                        |
| (vi)   | 489             | 323                                                                  | 230                                      | 44.3                              | 230                                      | 44.3                              | 0 %                             |

Continuing the prediction of features highly relevant to AgNP-water interaction, and to give fuller appreciation of surface attributes, a range of properties have been calculated (Methods) that includes: measures of the accessibility of surfaces and specific facets to water, surface area:volume ratios (SA:Vol) and nanoparticle roughness. It has been noted that the geometric curvature of the surface of very small particles controls the proportion and pattern of surface coverage of organic ligands (Walker et al., 2013); although water is a very small molecule, surface configuration and coverage will nevertheless be affected, particularly at the smaller size range, where particle dimensions are in the size range of the simulated probe (see Methods).



**Figure 4.** (a) Solvent Surface Area to Volume Ratio (probe radius = 1.4  $\text{\AA}$ ) (b) Contact Surface Area to Volume Ratio and (c) Fractal Dimension.

There are several different ways of defining nanoparticle surfaces, and these will have a consequent impact on properties such as surface area to volume ratio (SA:Vol), which in turn will correlate with AgNP reactivity. Data for two methods (solvent surface and the contact

surface, see Methods) are presented in Figure 4. The plots quantify important surface-property/size relationships for AgNPs, including the expected very high SA:Vol for the smaller AgNPs (<2000 atoms), (Figure 4a and 4b). Generally, SA:Vol ratio would be expected to scale as  $N^{-1/3}$ , where  $N$ =Number of atoms. The SA:Vol ratio for the solvent surface and contact surface scale as  $N^{-0.335}$  and  $N^{-0.254}$  respectively indicating that the size-dependence surface properties for small NPs depends on how the surface is probed (which, in turn, defines the appropriate method to measure surface effects). We now quantify the fractal-dimension of the smallest nanoparticles shown in Figure 4c and discuss the outcome in greater detail.

An associated important surface property for NP-ligand interactions, and potential reactivity and toxicity, is the surface roughness. Several definitions of surface roughness are available for large surfaces where the direction normal to the surface is well defined, but the definition is problematical for molecular scale particles. Following a number of biochemical/biophysical studies (Lewis and Rees, 1985; Renthall, 1999; Kaczor et al., 2012), we have used the surface fractal dimension as a proxy for roughness at the nanoscale. Data for the surface fractal dimension is also presented in Figure 4. The fractal dimension peaks around 7000-8000 atoms, corresponding to the largest of the truncated-decahedral structures and some of the smaller truncated-octahedral structures. The trend is not completely smooth, with some significant small peaks evident (e.g. at 1687 and 4579 atoms), but these do not coincide with the clusters that yielded the anomalous surface energies, suggesting that the surface roughness is not strongly affected by boundaries between different crystalline domains.

Reviewing the data presented above, we note that because the probability of ligands sticking to single crystal metal surfaces is higher for atomically rough planes, these predictions of relative roughness point toward an increased affinity for ligands (biochemical or otherwise) of the

AgNPs of sizes ranging between 1687-12195 atoms (approx. 1-6nm), peaking at around 8000 atoms. Additionally, AgNPs with highest surface fractal dimension  $D_f$  (circa 2.1nm) are structures with higher surface irregularities, occurring within the range of  $D_f$  values exhibited by transmembrane helices, water-soluble helices (Renthal, 1999) and by G protein-coupled receptors (Kaczor et al., 2012), but differing from the larger  $D_f$  exhibited by some other biologically important enzymes and proteins, for which  $2.3 \leq D_f \leq 2.5$  (Lewis and Rees, 1985). This may have important implications for cell uptake of nanoparticles within this size range. Structural roughness is important in biology. Irregular surfaces form more stabilizing contacts, allowing a greater number of van der Waals bonds in a given region than smoother surfaces. The probability of ligands sticking to single crystal metal surfaces is, in general, higher for atomically rough planes (Walker et al., 2013). This work thus predicts particular peak-affinity for ligands to AgNPs of sizes ranging around 8000 atoms.

Predictions of size effects on faceting, roughness and surface-curvature being maximised in small particles link to a number of studies addressing the effect of size on AgNP reactivity. However, no study, to our knowledge, presents a significant enough range of nanoparticle sizes that would enable sufficient comparison with our simulations. Despite the apparent limitation, this clearly demonstrates the need for computational approaches such as the one presented here. To circumvent this limitation, we have investigated the literature for review studies, which will give us a larger experimental dataset to use for our comparisons, with the understanding that across-dataset consistency of such reviews may be a limitation. Johnston et al (Johnston et al., 2010). survey of a large range of studies on Ag/AuNPs, concluded that size influences NP behaviour, with smaller particles showing a wider tissue distribution, further skin/intestine penetration, greater internalisation and higher toxicity. Although starting at 1.2 nm, the size-

range in that review was mostly 10-200 nm and the studies included covered 3-4 sizes, mostly tens of nms apart. Although not sufficiently systematic, the trends towards higher reactivity for smaller particles were consistent. Based on experiments, one therefore would predict an overall higher reactivity for smaller sizes, although the granularity of data and paucity at the size range of interest (1-6 nm) would not allow further comparisons. A number of studies (e.g. Peretyazhko et al., 2014; Ma et al., 2012) discuss size effects of Ag NPs (1-4nm) on dissolution and report higher intensity around this smaller size range, without however presenting enough detail to compare with our simulations. Notably, a study by Pan et al (Pan et al., 2007), also focussing on the smaller size range (0.8-15 nm), stated that 1.4 nm gold NPs were more toxic to cells than 1.2 nm gold NPs. This observation was however disputed (Johnston et al., 2010) based on the facts that the difference in size was extremely small and that the particles were derived from two alternative sources. Without disagreeing with this assessment on evidence basis, we could speculate that the computational variation in surface reactivity predicted here, would make the interpretation of Pan et al. plausible.

Further evidence for the role of surface reactivity comes from George et al. (George et al., 2012), who studied a range of AgNP shapes and concluded that the highest toxicity was not the result of greatest release of ionic Ag, but, instead, the presence of surface defects as demonstrated by high-resolution transmission electron microscopy. A concern when interpreting the results of studies based on small numbers of materials (5 in this case) is that it could be interpreted as showing that variations in surface reactivity are random and therefore each nanomaterial needs to be tested individually for toxicity. Interestingly, the authors discussed the need to develop combinatorial nanomaterial libraries that would allow a systematic study of surface defects. We would argue that, along with additional experimental data, computational

approaches can resolve the need for individual testing, although cross comparison with well-designed combinatorial libraries would be essential; however once established, computations can assist ‘safety-by-design’, being easily extended and transferable across all material types, nanostructures & chemistries without predictive paradigms restricted to, and by, evaluation of single non-transferable attributes at a time.

This study predicts surface structures/energetics of AgNPs and shows how water affects the transformation of the nanoparticle surfaces, by modifying their atomic configurations, and thus altering their potential for transport, fate, and toxicity. The work shows that size, at the lower range of the nanoscale, has a fundamental impact on nanoparticle behaviour, affecting surface energy and structural stability. The smaller nanoparticle size range of 1-6nm is predicted to be substantially more reactive than larger sizes, although this is not a simple function of size but incorporates also morphology. Once AgNPs exceed 6nm and having acquired a stable icosahedral structure, their reactivity no longer varies with size. The results presented go on to show that the presence of water generally favours interaction with the less stable and potentially more reactive AgNP surfaces and thus modifies the stability predicted *in vacuo*. Although not modelled here, biomolecules (e.g. proteins) would further contribute to surface structural transformations in nanoparticles that should complement future model development. The work demonstrates the potential of simulations to underpin any future nanomaterials safety framework, by providing fast and experimentally unbiased predictions of reactivity. The data presented here could contribute to the body of work aiming to identify reliable and/or sensitive descriptors for input into quantitative nanostructure-activity relationship models (nanoQSARs) with the ultimate aim to deliver predictive capability of nanomaterial behaviour to regulators and industry.

### **Conflicts of interest**

There are no conflicts to declare.

### **Author Contributions**

The manuscript was written through contributions of all authors. All authors have given approval to the final version of the manuscript.

### **Acknowledgments**

This work was supported by the European Union Seventh Framework Programme (FP7/2007-2013) under grant agreement 266712 (ModNanoTox). Financial support from Marie Skłodowska-Curie Individual Fellowship (NanoLabels 750455) under the European Union's Horizon 2020 research program is also appreciated. We thank Professor S. C. Parker of the University of Bath for the provision of the METADISE code. Professor Iseult Lynch for a critical review of the manuscript. Additionally, we acknowledge the provision of computer time on the (high performance computing) blueBEAR cluster of the Birmingham Environment for Academic Research at the University of Birmingham and EPSRC owned HECToR/ARCHER high end resource. We dedicate this paper to the memory of our co-author Mark Rodger, who, very sadly, didn't live to see it published.

### **References**

Accelrys Software Inc., D.S.M.E., Release 3.1, San Diego, 2013.

Barnard, A., 2010. Modelling of nanoparticles: approaches to morphology and evolution. Rep. Prog. Phys. 73, 086502.

- Barako, M.T., Gambin, V., Tice, J., 2018. Integrated nanomaterials for extreme thermal management: a perspective for aerospace applications. *Nanotechnology* 29, 154003.
- Berhanu, D., Valsami-jones, E., 2012. Nanotoxicity: are we confident for modelling?—An experimentalist's point of view. *Towards Efficient Designing of Safe Nanomaterials*, pp. 54-68.
- Briffa, S.M., Nasser, F., Valsami-Jones, E., Lynch, I., 2018. Uptake and Impacts of Polyvinylpyrrolidone (PVP) Capped Metal Oxide nanoparticles on *Daphnia magna*: role of core composition and acquired corona. *Environ. Sci.: Nano*. 5, 1745-1756.
- Day, T.J., Soudackov, A.V., Čuma, M., Schmitt, U.W., Voth, G.A., 2002. A second generation multistate empirical valence bond model for proton transport in aqueous systems. *J. Chem. Phys.* 117, 5839-5849.
- De Matteis, V., Malvindi, M.A., Galeone, A., Brunetti, V., De Luca, E., Kote, S., Kshirsagar, P., Sabella, S., Bardi, G., Pompa, P.P., 2015. Negligible particle-specific toxicity mechanism of silver nanoparticles: the role of  $\text{Ag}^+$  ion release in the cytosol. *Nanomed. Nanotechnol. Biol. Med.* 11, 731-739.
- Dong, F., Mohd Zaidi, N.F., Valsami-Jones, E., Kreft, J.U., 2017. Time-resolved toxicity study reveals the dynamic interactions between uncoated silver nanoparticles and bacteria. *Nanotoxicology* 11, 637-646.
- Durán, N.; Silveira, C. P.; Durán, M.; Martínez, D. S. T., Silver nanoparticle protein corona and toxicity: a mini-review. *Journal of Nanobiotechnology* **2015**, 13 (1), 55.
- Fadeel, B., Farcas, L., Hardy, B., Vázquez-Campos, S., Hristozov, D., Marcomini, A., Lynch, I., Valsami-Jones, E., Alenius, H., Savolainen, K., 2018. Advanced tools for the safety assessment of nanomaterials. *Nat. Nanotechnol.* 13, 537-543.



Ge, C., Fang, G., Shen, X., Chong, Y., Wamer, W.G., Gao, X., Chai, Z., Chen, C., Yin, J.-J., 2016. Facet energy versus enzyme-like activities: the unexpected protection of palladium nanocrystals against oxidative damage. *ACS nano* 10, 10436-10445.

George, S., Lin, S., Ji, Z., Thomas, C.R., Li, L., Mecklenburg, M., Meng, H., Wang, X., Zhang, H., Xia, T., 2012. Surface defects on plate-shaped silver nanoparticles contribute to its hazard potential in a fish gill cell line and zebrafish embryos. *ACS nano* 6, 3745-3759.

Hoover, W.G., 1985. Canonical dynamics: equilibrium phase-space distributions. *Phys. Rev. A* 31, 1695.

Johnston, H.J., Hutchison, G., Christensen, F.M., Peters, S., Hankin, S., Stone, V., 2010. A review of the in vivo and in vitro toxicity of silver and gold particulates: particle attributes and biological mechanisms responsible for the observed toxicity. *Crit. Rev. Toxicol.* 40, 328-346.

Kaczor, A.A., Guixà-González, R., Carrió, P., Obiol-Pardo, C., Pastor, M., Selent, J., 2012. Fractal dimension as a measure of surface roughness of G protein-coupled receptors: implications for structure and function. *J. Mol. Model.* 18, 4465-4475.

Khan, F.R., Paul, K.B., Dybowska, A.D., Valsami-Jones, E., Lead, J.R., Stone, V., Fernandes, T.F., 2015. Accumulation dynamics and acute toxicity of silver nanoparticles to *Daphnia magna* and *Lumbriculus variegatus*: implications for metal modeling approaches. *Environ. Sci. Technol.* 49, 4389-4397.

Lartigue, L.n., Hugounenq, P., Alloyeau, D., Clarke, S.P., Lévy, M., Bacri, J.-C., Bazzi, R., Brougham, D.F., Wilhelm, C., Gazeau, F., 2012. Cooperative organization in iron oxide multi-core nanoparticles potentiates their efficiency as heating mediators and MRI contrast agents. *ACS nano* 6, 10935-10949.

- Lee, B.-J., Shim, J.-H., Baskes, M., 2003. Semiempirical atomic potentials for the fcc metals Cu, Ag, Au, Ni, Pd, Pt, Al, and Pb based on first and second nearest-neighbor modified embedded atom method. *Phys. Rev. B* 68, 144112.
- Levard, C., Hotze, E.M., Lowry, G.V., Brown Jr, G.E., 2012. Environmental transformations of silver nanoparticles: impact on stability and toxicity. *Environ. Sci. Technol.* 46, 6900-6914.
- Lewis, M., Rees, D.C., 1985. Fractal surfaces of proteins. *Science* 230, 1163-1165.
- Li, Y., Zhao, J., Shang, E., Xia, X., Niu, J., Crittenden, J., 2017. Effects of chloride ions on dissolution, ROS generation, and toxicity of silver nanoparticles under UV irradiation. *Environ. Sci. Technol.* 52, 4842-4849.
- Liu, N., Li, K., Li, X., Chang, Y., Feng, Y., Sun, X., Cheng, Y., Wu, Z., Zhang, H., 2016. Crystallographic facet-induced toxicological responses by faceted titanium dioxide nanocrystals. *ACS nano* 10, 6062-6073.
- Lynch, I., Afantitis, A., Leonis, G., Melagraki, G., Valsami-Jones, E., 2017. Strategy for identification of nanomaterials' critical properties linked to biological impacts: interlinking of experimental and computational approaches. *Advances in QSAR Modeling*. Springer, pp. 385-424.
- Lynch, I., Dawson, K.A., Lead, J.R., Valsami-Jones, E., 2014a. Macromolecular coronas and their importance in nanotoxicology and nanoecotoxicology. *Frontiers of Nanoscience*. Elsevier, pp. 127-156.
- Lynch, I., Weiss, C., Valsami-Jones, E., 2014b. A strategy for grouping of nanomaterials based on key physico-chemical descriptors as a basis for safer-by-design NMs. *Nano Today* 9, 266-270.

- Marks, L., 1983. Modified Wulff constructions for twinned particles. *J. Cryst. Growth* 61, 556-566.
- Ma, R., Levard, .C., Marinakos, S.M., Cheng, Y., Liu, J., Michel, F.M., Brown Jr, G.E., Lowry, G.V., 2012. Size-Controlled Dissolution of Organic-Coated Silver Nanoparticles. *Environ. Sci. Technol.* 46, 752-759.
- Maynard, A.D., 2014. Is novelty overrated? *Nat. Nanotechnol.* 9, 409.
- Medasani, B., Park, Y.H., Vasiliev, I., 2007. Theoretical study of the surface energy, stress, and lattice contraction of silver nanoparticles. *Phys. Rev. B* 75, 235436.
- Monopoli, M.P., Åberg, C., Salvati, A., Dawson, K.A., 2012. Biomolecular coronas provide the biological identity of nanosized materials. *Nat. Nanotechnol.* 7, 779.
- Nafisi, S., Maibach, H., 2017. *Nanotechnology in cosmetics. Cosmetic Science and Technology: Theoretical Principles and Applications*, Elsevier, 337.
- Nanda, K., Kruis, F., Fissan, H., 2002. Evaporation of free PbS nanoparticles: evidence of the Kelvin effect. *Phys. Rev. Lett.* 89, 256103.
- Nanda, K., Maisels, A., Kruis, F., Fissan, H., Stappert, S., 2003. Higher surface energy of free nanoparticles. *Phys. Rev. Lett.* 91, 106102.
- Nosé, S., 1984. A unified formulation of the constant temperature molecular dynamics methods. *J. Chem. Phys.* 81, 511-519.
- Pan, Y., Neuss, S., Leifert, A., Fischler, M., Wen, F., Simon, U., Schmid, G., Brandau, W., Jahn-Dechent, W., 2007. Size-dependent cytotoxicity of gold nanoparticles. *Small* 3, 1941-1949.

- Pereda, M., Marcovich, N., Ansorena, M., 2018. Nanotechnology in Food Packaging Applications: Barrier Materials, Antimicrobial Agents, Sensors, and Safety Assessment. Handbook of Ecomaterials. Springer, pp. 1-22.
- Peretyazhko, T.S., Zhang, Q.B., Colvin, V.L., 2014. Size-controlled dissolution of silver nanoparticles at neutral and acidic pH conditions: kinetics and size changes. Environ. Sci. Technol. 2014, 48, 11954-11961.
- Perkins, R., Fang, H., Tong, W., Welsh, W.J., 2003. Quantitative structure-activity relationship methods: Perspectives on drug discovery and toxicology. Environ. Toxicol. Chem. 22, 1666-1679.
- Renthal, R., 1999. Transmembrane and water-soluble helix bundles display reverse patterns of surface roughness. Biochem. Biophys. Res. Commun. 263, 714-717.
- Schmitt, U.W., Voth, G.A., 1999. The computer simulation of proton transport in water. J. Chem. Phys. 111, 9361-9381.
- Smith, W., Forester, T., 1996. DL\_POLY\_2. 0: A general-purpose parallel molecular dynamics simulation package. J. Mol. Graphics 14, 136-141.
- Sutton, A., Chen, J., 1990. Long-range finnis–sinclair potentials. Philos. Mag. Lett. 61, 139-146.
- TobyáKelsey, E., áde Leeuw, N.H., 1996. Atomistic simulation of dislocations, surfaces and interfaces in MgO. J. Chem. Soc., Faraday Trans. 92, 433-438.
- Todd, B., Lynden-Bell, R., 1993. Surface and bulk properties of metals modelled with Sutton-Chen potentials. Surf. Sci. 281, 191-206.
- Varty, Z., 2017. Simulated Annealing Overview.
- Walczyk, D., Bombelli, F.B., Monopoli, M.P., Lynch, I., Dawson, K.A., 2010. What the cell “sees” in bionanoscience. J. Am. Chem. Soc. 132, 5761-5768.

Walker, D.A., Leitsch, E.K., Nap, R.J., Szleifer, I., Grzybowski, B.A., 2013. Geometric curvature controls the chemical patchiness and self-assembly of nanoparticles. *Nat. Nanotechnol.* 8, 676.

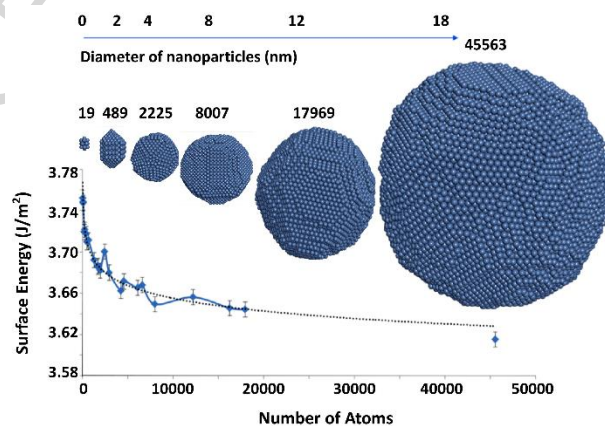
Wang, B., Liu, M., Wang, Y., Chen, X., 2011. Structures and energetics of silver and gold nanoparticles. *J. Phys. Chem. C* 115, 11374-11381.

Wang, J., Wolf, R.M., Caldwell, J.W., Kollman, P.A., Case, D.A., 2004. Development and testing of a general amber force field. *J. Comput. Chem.* 25, 1157-1174.

Zhang, P., Xie, C.J., Ma, Y.H., He, X., Zhang, Z.Y., Ding, Y.Y., Zheng, L.R., Zhang, J., 2017. Shape-dependent transformation and translocation of ceria nanoparticles in cucumber plants. *Environ. Sci. Technol. Lett.* 4, 380-385.

Zhu, M., Nie, G., Meng, H., Xia, T., Nel, A., Zhao, Y., 2012. Physicochemical properties determine nanomaterial cellular uptake, transport, and fate. *Acc. Chem. Res.* 46, 622-631.

## Graphic abstract



### Highlights

1. Morphological transformation as a function of size was simulated.
2. Significant change in exposed facets can occur while size varies undetectably.
3. Water affects the surface morphology of Ag nanoparticles.

ACCEPTED MANUSCRIPT